Surface charge measurements and (dis)charging dynamics of organic semiconductors in various media using optical tweezers

Rebecca R. Grollman, Kyle Peters, and Oksana Ostroverkhova

Department of Physics, Oregon State University, Corvallis, OR 97331

ABSTRACT

An exciting application of optical tweezers is the measurement of the surface charge on a trapped particle, as well as its time evolution with a single charge resolution. We report on an optical tweezer-based method to measure the effective surface charge on an organic semiconductor film at microscopic scales, which offers opportunities for investigations of ion and electron transfer between organic molecules and surrounding medium. Effective charge densities of 13±5 elementary charges per μm^2 were observed in anthradithiophene-coated silica microspheres suspended in water, with a more than an order of magnitude reduction in charge densities upon replacing water with the 50% wt/wt glycerol/water mixture.

Keywords: Optical tweezers, effective charge, organic semiconductors, charging dynamics

1. INTRODUCTION

Organic semiconductors are of interest due to their low cost, easy fabrication, and tunable properties for applications in thin-film transistors, light-emitting diodes, solar cells, etc.[1] As most applications rely on (photo)conductive properties, which depend on the ability of the molecule to accept or donate an electron, it is important to understand how these properties are affected by the molecular structure, packing in the film, and surrounding environment. Most methods currently used for probing charge generation and transport in molecular systems utilize thin films made of molecules of interest incorporated in device structures. The device characterization often yields a convolution of molecular properties with those imposed by restrictions of the device geometry, making it difficult to establish intrinsic properties of the molecules. Our quest is to develop the ability to probe intrinsic behavior of the molecular charge during conduction, as well as to assess charge exchange between the molecule and surrounding media at nanoscales, depending on the local environment.

Optical tweezers have been extensively used in many applications spanning chemistry, biology, engineering, and physics.[2] With optical tweezers, a laser beam focused with a high numerical aperture (NA) lens is used to optically trap and manipulate particles on sub-micron scales. Recently, an optical tweezer-based technique that enabled measurement of a surface charge density of microscopic particles suspended in liquids was reported, and resolution of a single electron charge (e) was demonstrated.[3] Further development of this technique led to measurements of single (dis)charging events on a 1 μm PMMA sphere in a non-polar liquid (dodecane).[4] In this paper, we apply an optical tweezer-based method to studies of charging of organic semiconductor molecules in various environments and extend the method to enable measurements of (dis)charging under photoexcitation.

2. MATERIALS AND METHODS

2.1 Materials and Sample Preparation

For our initial experiments, we chose a fluorinated anthradithiophene (ADT) derivative functionalized with triethylsilylethynyl (TES) side groups, ADT-TES-F. Thin films of this derivative have shown thin-film transistor charge carrier mobilities of 1.5 $cm^2/(Vs)$,[5] fast charge carrier photogeneration,[6,7] and high photoconductivity under continuous wave (cw) illumination.[8] Amorphous silica spheres 1 μm in diameter (Thermo Scientific, 0.99±0.02 μm, refractive index n = 1.40-1.46, 2% suspension in water) were coated with ADT-TES-F molecules as follows. A 2 μL solution of silica spheres in water was added to 50 μL 30 mM stock solution of ADT-TES-F in toluene and sonicated for 20 minutes. Then, 14 μL of the mixture was added to 4 mL of ultra-pure millipore (Milli-Q, 18 $M\Omega$ cm) water, sonicated for 5 minutes, and left unperturbed overnight. While most charge

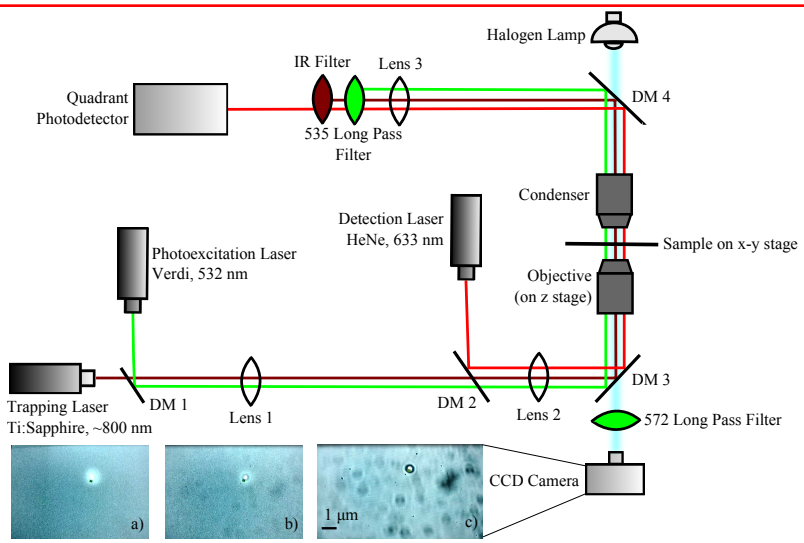

Figure 1. The experimental set up used to measure effective charge, which includes a trapping laser (800 nm), detection laser (633 nm), and photoexcitation laser (532 nm) for the ADT-TES-F-coated spheres. The images are of a trapped ADT-TES-F coated silica sphere: a) under 532 nm excitation (halogen lamp off), b) under 532 nm excitation (halogen lamp on), and c) no excitation (halogen lamp on). Fluorescence emission of the ADT-TES-F coating can be seen in a) and b).

measurements with optical tweezers have been done using nonpolar solvents,[3,4,9,10] our choice of millipore water for the initial set of experiments was dictated by solubility of ADT-TES-F in many typical nonpolar solvents, which would compromise quality of the coating. The ADT-TES-F coating was confirmed using fluorescence microscopy at 532 nm cw excitation, which resulted in strong emission by ADT-TES-F molecules at wavelengths of >580 nm (Fig. 1).[8] No fluorescence was observed from uncoated silica spheres. As control samples, we used uncoated silica spheres and 1 μm in diameter polystyrene (PS) spheres (Duke Scientific, Inc., refractive index n = 1.55). We also prepared silica spheres coated with PS, for which 2 μL solution of silica spheres in water was added to 40 μL of 1% wt/wt solution of PS in toluene followed by the same protocol used for coating silica spheres with ADT-TES-F. Additionally, we prepared solutions of ADT-TES-F coated silica spheres in a 50% wt/wt mixture of water and glycerol by adding 4 μL of the coated sphere solution in toluene to 4 mL of the 50% wt/wt mixture of water and glycerol.

Solution of spheres in millipore water or water/glycerol solution prepared as described above was added to the sample holder shown in Fig. 2. Sample holders were constructed by grinding two holes into a glass slide to insert the solution of interest, and creating a fluid chamber with small pieces of a glass coverslip secured with UV glue (Thorlabs, NOA81). The top glass coverslip had two pieces of aluminum foil (secured with UV glue), which served as coplanar electrodes. The electrodes were separated by a gap of approximately 100 μm measured in each sample using optical microscopy by moving the sample on an x-y stage between the two electrodes and recording the position of the electrodes using a micrometer. Spheres were typically trapped about 20 μm away from the top coverslip to avoid any interactions between the glass slide and sphere. Spheres were trapped in the center of the gap between two electrodes to minimize edge effects.

2.2 Optical Tweezer Trapping Setup

Optical tweezer trapping was performed in a custom inverted microscope assembly with an oil immersion microscope objective (Edmund Optics, 100X, NA of 1.25, 160 mm tube length) as shown in Fig. 1.[11] Spheres were trapped with a cw 800 nm Ti:Sapphire laser (KM Labs, Inc.). The position of a trapped sphere was detected by the scattering of a 633 nm Helium-Neon laser collected into a Hamamatsu S4349 quadrant photodiode (QPD). The QPD signal was collected using a data acquisition card (DAQ) (NI-6221), and data acquisition was done using a custom LabView program. Additionally, a cw 532 nm laser beam (Verdi V5, Coherent, Inc.), collimated

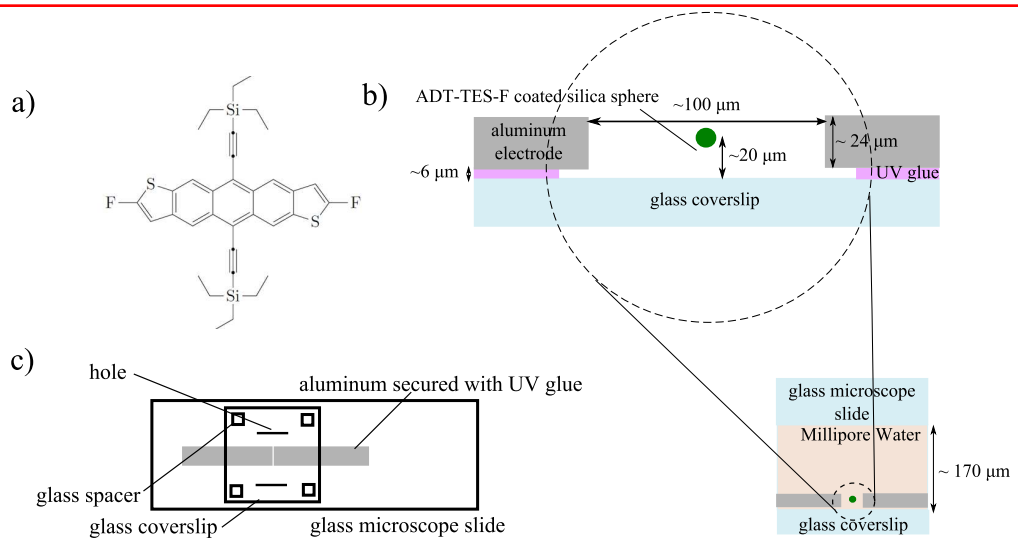

Figure 2. a) Molecular structure of ADT-TES-F. b) Side view of sample holder. Note the trapping distance away from the glass coverslip to minimize interaction between the coverslip and sphere. c) Top view of sample holder to show the holes ground into the microscope slide and positioning of the electrodes.

to minimize its effect on the trap stability, was used to photoexcite ADT-TES-F in ADT-TES-F-coated spheres. Spheres were imaged with a CCD camera and halogen lamp. When assessing fluorescence from an ADT-TES-F coating, a long-pass 572 nm filter was placed in front of the CCD camera to transmit the fluorescence emission of the ADT-TES-F molecules, while blocking the 532 nm excitation. Filters were also placed in front of the QPD to block the 800 nm and 532 nm light.

2.3 Trap stiffness measurements

A trapped sphere can be treated as an object attached to a spring with a spring constant or, in our case, a trap stiffness k. We assumed that the force acting on the sphere when it is displaced small distances from the equilibrium in the x-y plane (perpendicular to the trapping beam propagation direction) can be described by the Hooke's law. The trap stiffness in the x-y plane was calculated by applying four analysis methods to the data.[11] In a stable unperturbed trap, the trap stiffness values extracted from each method are equal within approximately 10-15%. The methods included applying the equipartition theorem to the variance of the sphere's motion in the trap, performing a Gaussian fit to a histogram of the sphere's position in the trap, obtaining the corner frequency of the power spectrum of the suppressed Brownian motion of the sphere, and fitting the data with the parabolic function describing the potential well. For example, through the variance in the particle's displacement σ^2, the trap stiffness can be calculated using the equipartition theorem,

$$\frac{1}{2}k\sigma^2 = \frac{1}{2}k_B T, \tag{1}$$

where k_B is the Boltzmann constant and T is temperature.[11] Trap stiffness can also be calculated from the power spectrum of the position fluctuations given by

$$|\tilde{x}(f)^2| = \frac{k_B T}{\pi^2 \beta (f_c^2 + f^2)}, \tag{2}$$

where f is the frequency, β is the drag coefficient of the sphere in the medium, and f_c is the corner frequency. In particular, the corner frequency is related to the trap stiffness as $f_c = k/(2\pi\beta)$,[11] from which the trap stiffness is readily obtained.

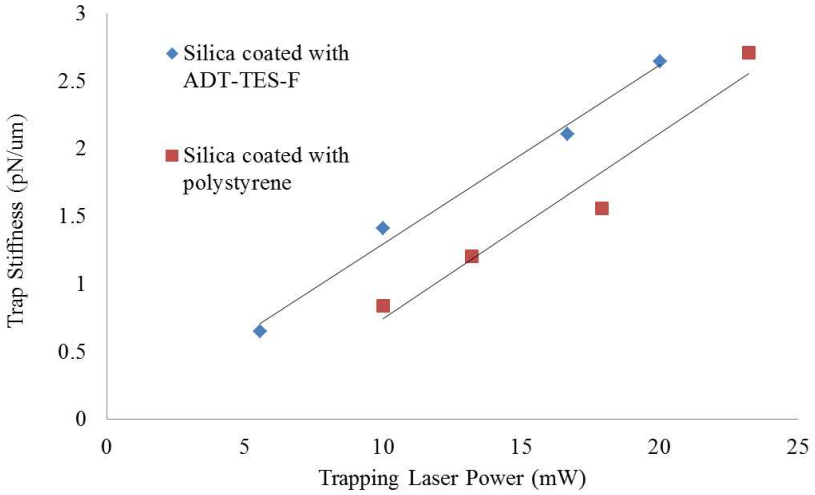

Figure 3. Dependence of measured trap stiffness on the trapping beam power in coated spheres. Linear dependence is expected in the case of stable trapping.

The trap stiffness was also measured at various trapping beam powers, and the linear dependence of k on the power was observed (Fig. 3). As expected, at same trapping beam power, the trap stiffness for PS spheres, as well as for PS- and ADT-TES-F-coated spheres, was higher than that for silica spheres since PS and ADT-TES-F have a higher index of refraction as compared to silica.[11]

2.4 Charge Measurements

When an applied AC electric field is added to a trapped sphere, an electric field-dependent component $|\tilde{x}(f)^2|_E$ is added to the power spectrum from Eq. (2) to become

$$|\tilde{x}(f)^2| = \frac{k_B T}{\pi^2 \beta (f_c^2 + f^2)} + \frac{k_B T \gamma^2}{2k}[\delta(f - f_{AC})], \tag{3}$$

where γ^2 is the scaled ratio of the mean square periodic and Brownian forces and can be calculated from

$$P_{AC} = \int_{-\infty}^{\infty} |\tilde{x}(f)^2|_E df = \frac{k_B T}{k}\gamma^2, \tag{4}$$

where $|\tilde{x}(f)^2|_E$ is the power spectrum due to the applied electric field.[3] As shown in Ref. 3 the effective charge Z_{eff} on a sphere can be calculated with

$$e|Z_{eff}| = \frac{\gamma\beta}{E}\sqrt{\frac{2k_B T}{k}((2\pi f_{AC})^2 + (k/\beta))}, \tag{5}$$

where e is the charge of an electron, E is the applied electric field, and f_{AC} is the driving frequency of the electric field.

To measure effective charge on our spheres, we applied an AC voltage in the range of 2.5 V_{pp} to 20 V_{pp} across the electrodes of the sample holder using an amplified sinusoidal signal from function generator (Tektronix, AFG3021). Frequencies f_{AC} ranging from 30 Hz to 500 Hz were tested, and charge measurements at frequencies in the range between 70 and 110 Hz yielded most consistent data, prompting us to select a driving frequency of 110 Hz for most experiments reported here. The electric field was estimated as $\lambda\frac{V}{d}$ where V is the applied voltage and d is the distance between electrodes. The scaling factor λ, described in Ref. 3, takes into account the

electric field dependence on the position of the sphere with respect to the electrodes. In order to probe changes in effective charge density upon photoexcitation of ADT-TES-F in ADT-TES-F-coated spheres, we performed charge measurements under 532 nm excitation at powers of up to 28 mW.

Another method to measure the effective charge of spheres using optical tweezers, which also enables measurements of (dis)charging dynamics, uses a much higher sampling frequency, higher applied electric field, and higher driving frequency. Then, the effective charge can be calculated using[4]

$$|Z_{eff}| = \frac{2\beta f_{s,Q}}{E}\left(2\pi f_c Re(|\tilde{x}(f)^2|_E) + 2\pi f_{AC} Im(|\tilde{x}(f)^2|_E)\right), \quad (6)$$

where $f_{s,Q}$ is the sampling rate of overlapping windows of charge measurements within a data set. To measure the effective charge with this method, we increased our sampling frequency to 20 kHz and used f_{AC}=1 kHz and $f_{s,Q}$=4.88 Hz.

3. RESULTS AND DISCUSSION

An example of data obtained from a PS sphere at a trapping power of 16.5 mW at several applied electric fields is shown in Fig. 4. While Gaussian distribution of the sphere position in the trap was observed at low electric fields, it gradually changed to the bimodal distribution (e.g. at 34.3 kV/m in Fig. 4, bottom). This is indicative of a presence of charge on the sphere surface and is due to a partial trap destabilization by a force exerted by the applied electric field on the surface charge. In this case, the suppressed Brownian motion of a trapped sphere is replaced by a sinusoidal time dependence of the sphere position, following that of the applied electric field. The data in Fig. 4 are consistent with findings of Ref. 3, which predicted the bimodal distribution at values of γ of Eq. 4 greater than 1.257. In Fig. 4, γ is 0.83 and 1.75 for electric fields of 17.1 kV/m (middle) and 34.3 kV/m (bottom), respectively.

The measurements of the effective charge were conducted at low applied electric fields, at which the trap destabilization effects were negligible. Table 1 shows effective surface charge densities obtained in silica, PS, and silica coated with either PS or ADT-TES-F. It is well known that silica in contact with water is negatively charged due to dissociation of silanol groups.[12] The magnitude of the effective charge density increases with ionic strength.[12] In ultra-pure deionized water with an ionic strength of below 10^{-6}M, it is expected to be below 2000 $e/\mu m^2$, where e is the elementary charge. For example, a surface charge density of -700 $\pm$ 150 $e/\mu m^2$ was obtained in Ref. 12. Our experiments yielded the magnitude of the surface charge density for silica spheres of about 290 $e/\mu m^2$ (Table 1). This value represents a lower bound on the magnitude of the surface charge density, as the electric field in the proximity to the sphere immersed in a medium with high dielectric constant such as water ($\epsilon = 81$) is partially screened; accounting for such reduction in the electric field in the Eq. 5 would increase the effective charge Z_{eff}.

Negative charge on the surface of PS spheres in water has previously been attributed to the adsorption of hydroxyl ions (ion transfer), to the electron transfer from water to PS resulting from the overlap of local intrinsic molecular-ion states in PS and water, or both.[13,14] The obtained surface charge densities ranged from 455 $e/\mu m^2$ to 553 $e/\mu m^2$ for PS spheres functionalized with sulfate groups and carboxylated, respectively[15] and 9375 $e/\mu m^2$ for larger PS spheres (d=2.23 μm) in an aqueous solution of 1-butyl-3-methylimidazolium chloride (BMIM-CI) at a pH of 6.[16] Surface charge densities for PS spheres obtained in our experiments in ultra-pure water yielded considerably lower values (Table 1), as expected.

The silica spheres coated with PS exhibited surface charge densities lower than those in uncoated silica spheres and higher than those in PS spheres (Table 1). Adsorption of PS by silica has been previously observed and attributed to a hydrogen bond formation between the hydroxyl group on silica and phenyl ring on PS.[17] Therefore, a reduction of effective charge in PS-coated silica spheres by a factor of ~3, as compared to uncoated silica spheres, is due to a partial or complete isolation of the silanol groups on the silica surface from water, which prevents their dissociation. The silica spheres coated with ADT-TES-F exhibited effective charge densities that are a factor of ~20 lower than those in uncoated silica and a factor of ~7 lower than those in silica coated with PS. ADT-TES-F is a nonpolar molecule which is not expected to significantly interact with water, and the observed effective charge reduction reflects efficient adsorption of ADT-TES-F onto silica surface, which prevents

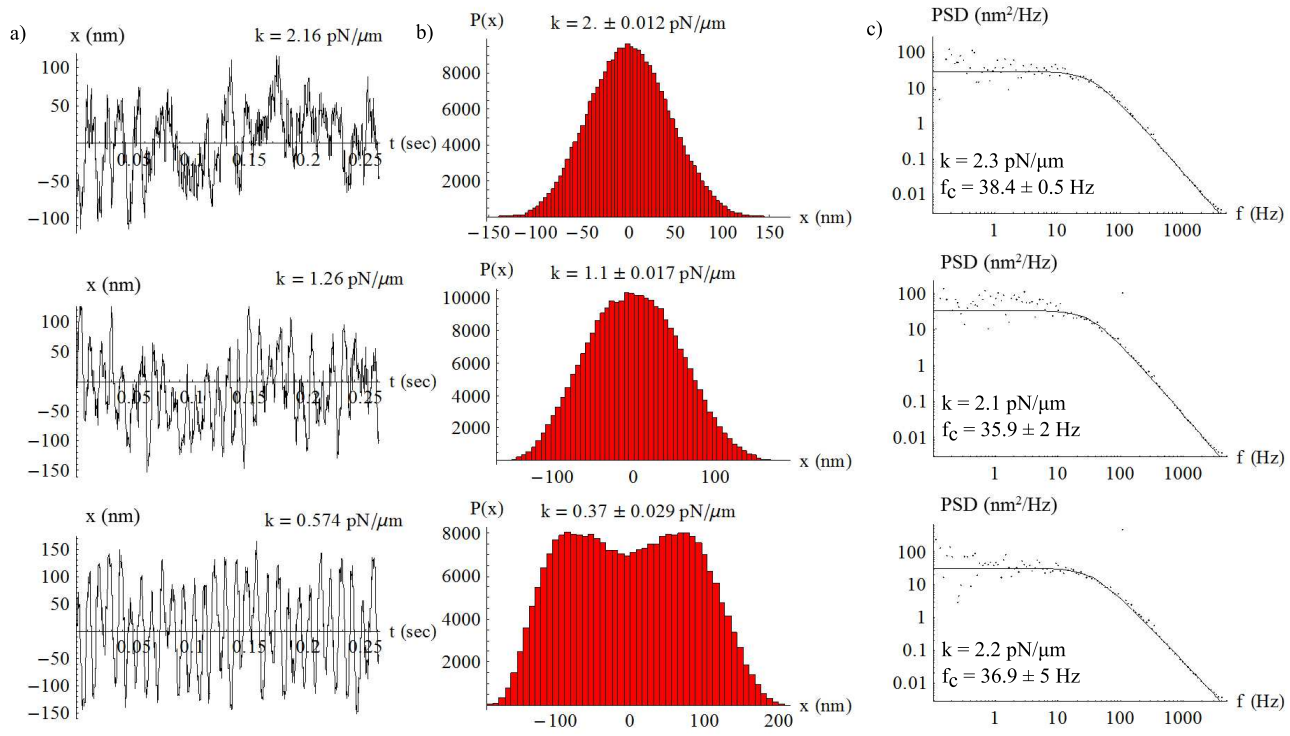

Figure 4. Example of data obtained from a trapped PS sphere: (top) no applied electric field, (middle) and (bottom) applied electric fields of 17.1 kV/m and 34.3 kV/m, respectively, with a driving frequency of 110 Hz. Note the peaks at 110 Hz in the power spectrum due electric field induced motion of the charged sphere. a) Time series data of suppressed Brownian motion. Note a transition to sinusoidal dependence at higher electric fields. b) Histogram of the sphere's motion in the trap. c) Power spectrum of the sphere's motion.

silica-water interaction. A considerably smaller effective charge densities in ADT-TES-F-coated as compared to PS-coated spheres are most likely due to efficient ADT-TES-F aggregation that promotes thicker surface layers. A further reduction by more than an order of magnitude in effective charge density was observed in the ADT-TES-F-coated silica spheres when water was replaced with a 50 % wt/wt mixture of water and glycerol, due to reduction in polarity ($\epsilon = 64$). This is consistent with Ref. 15 who found more than an order of magnitude reduction in the effective charge of PS spheres in 35% wt/wt glycerol/water solution as compared to water.

In order to investigate time evolution of effective charge density, we increased the AC electric field driving frequency to 1 kHz, which is substantially higher than the typical corner frequencies characterizing our optical traps (Figs. 4(c) and 5(a)), and analyzed data obtained from ADT-TES-F-coated silica spheres in a 50 % wt/wt water/glycerol mixture using Eq. 6 and a method proposed in Ref. 4. Rapid fluctuations of the effective charge were observed, which are expected in a polar medium; however, considerably higher electric fields are necessary to quantify time dependence of the charge density. Similarly, considerably higher applied electric fields are needed to observe a time evolution of effective charge as a result of photoconductivity induced in the ADT-TES-F film by the 532 nm excitation under applied electric field, as no effect of ADT-TES-F photoexcitation with cw 532 nm beam on the effective charge density was observed under our experimental conditions.

4. CONCLUSIONS

We demonstrated feasibility of using an optical tweezer-based technique for measurements of effective charge density in organic semiconductor films at microscopic scales in several environments.Effective charge densities of 13±5 elementary charges per μm^2 were observed in ADT-TES-F-coated silica microspheres suspended in water. These are about a factor of ∼7 lower than effective charge densities obtained in similar silica microspheres coated

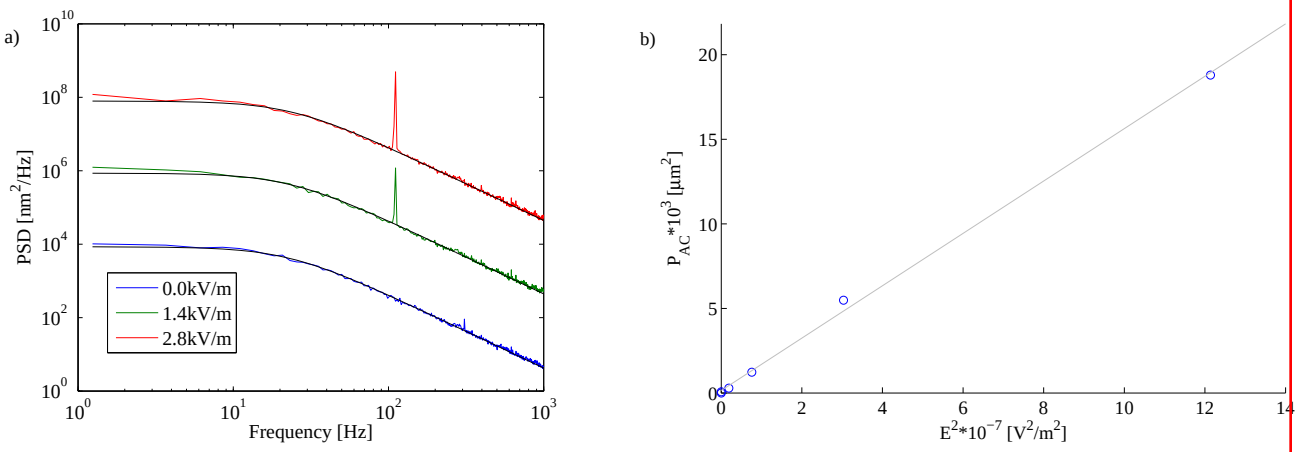

Figure 5. a) Power spectral density of a suppressed Brownian motion of a trapped silica sphere. The data at various applied electric fields have been shifted along y-axis for clarity. As the applied electric field increased, the peak height at the driving frequency of 110 Hz increased, in accordance with Eq. (3). b) P_{AC} of Eq. (4) extracted from data in a) as a function of an applied electric field squared. Linear fit, based on Eqs. (4) and (5), is also shown.

Table 1. Effective surface charge measured in various spheres in water. The values were averaged over 5-7 spheres of the same type and over at least 9 data runs for each sphere. The error bars reflect sphere-to-sphere variation. The run-to-run error for each given sphere was less than 5%.

Sphere Type	**Surface Charge (e/μm^2)**
Silica	290 ± 95
PS	25 ± 12
Silica coated with PS	90 ± 50
Silica coated with ADT-TES-F	13 ± 5

with PS, indicative of efficient adsorption of ADT-TES-F onto silica surface followed by ADT-TES-F aggregation to promote a thicker coating, as compared to PS. Effective charge densities lower than one elementary charge per μm^2 were observed in the ADT-TES-F-coated spheres upon replacing water with the 50% wt/wt glycerol/water mixture. The experimental technique was also extended to incorporate capability of measuring photoinduced changes in effective charge density which will next be applied for studies of photoinduced charge transfer and exciplex dissociation in organic semiconductors depending on the local environment.

ACKNOWLEDGMENTS

We thank Prof. J. E. Anthony for ADT-TES-F, Prof. D. H. McIntyre for providing data analysis software, and Jacob Busche for assistance in sample preparation. This work was supported in part by the National Science Foundation grant DMR-1207309.

REFERENCES

1. O. Ostroverkhova, ed., *Handbook of organic materials for optical and (opto)electronic devices*, Woodhead Publishing, Cambridge, U.K., 2013.
2. A. Ashkin, "History of optical trapping and manipulation of small-neutral particle, atoms, and molecules," *IEEE J. Sel. Top. Quantum Electron* **6**, pp. 841–856, 2000.
3. G. S. Roberts, T. A. Wood, W. J. Frith, and P. Bartlett, "Direct measurement of the effective charge in nonpolar suspensions by optical tracking of single particles," *J. Chem. Phys.* **126**, p. 194503, 2007.

4. F. Beunis, F. Strubbe, K. Neyts, and D. Petrov, "Beyond millikan: The dynamics of charging events on individual colloidal particles," *Physical Review Letters* **108**, p. 016101, 2012.
5. S. Park, D. A. Mourey, S. Subramanian, J. E. Anthony, and T. N. Jackson, "High-mobility spin-cast organic thin film transistors," *Applied Physics Letters* **93**, p. 043301, 2008.
6. J. Day, A. D. Platt, O. Ostroverkhova, S. Subramanian, and J. Anthony, "Organic semiconductor composites: influence of additives on the transient photocurrent," *Applied Physics Letters* **94**, p. 013306, 2009.
7. J. Day, A. Platt, S. Subramanian, J. Anthony, and O. Ostroverkhova, "Influence of organic semiconductor-metal interfaces on the photoresponse of functionalized anthradithiophene thin films," *Journal of Applied Physics* **105**, p. 103703, 2009.
8. A. D. Platt, J. Day, S. Subramanian, J. E. Anthony, and O. Ostroverkhova, "Optical, fluorescent, and (photo)conductive properties of high-performance functionalized pentacene and anthradithiophene derivatives," *Journal of Physical Chemistry C* **113**, pp. 14006–14014, 2009.
9. F. Strubbe, F. Beunis, and K. Neyts, "Determination of the effective charge of individual colloidal particles," *Journal of Colloid and Interface Science* **301**, pp. 302–309, 2006.
10. S. K. Sainis, V. Germain, C. O. Mejean, and E. R. Dufresne, "Electrostatic interactions of colloidal particles in nonpolar solvents: Role of surface chemistry and charge control agents," *Langmuir* **24**, pp. 1160–1164, 2008.
11. M. J. Kendrick, D. H. McIntyre, and O. Ostroverkhova, "Wavelength dependence of optical tweezer trapping forces on dye-doped polystyrene microscpheres," *J. Opt. Soc. Am. B* **26**, pp. 2189–2198, 2009.
12. S. H. Behrens and D. G. Grier, "The charge of glass and silica surfaces," *Journal of Chemical Physics* **115**, pp. 6716–6721, 2001.
13. A. A. Kamel, C. M. Ma, M. S. El-Aasser, F. J. Micale, and J. W. Vanderhoff, "Concerning the origin of charge at the polystyrene particle/water interface," *Dispersion Science and Technology* **263**, pp. 315–330, 1981.
14. L. S. McCarty, A. Winkleman, and G. M. Whitesides, "Electronic self-assembly of polystyrene microspheres by using chemically directed contact electrification," *Angew. Chem.* **119**, pp. 210–213, 2007.
15. N. Garbow, M. Evers, T. Palberg, and T. Okubo, "On the electrophoretic mobility of isolated colloidal spheres," *Journal of Physics: Condensed Matter* **16**, pp. 3835–3842, 2004.
16. M. M. Elmahdy, C. Gutsche, and F. Kremer, "Forces within single pairs of charged colloids in aqueous solutions of ionic liquids as studied by optical tweezers," *J. Phys. Chem. C* **114**, pp. 19452–19458, 2010.
17. S. K. Parida, S. Dash, S. Patel, and B. K. Mishra, "Adsorption of organic molecules on silica surface," *Advances in Colloid and Interface Science* **121**, pp. 77–110, 2006.